

Boundary Control for Wildfire Mitigation

M. C. Belhadjoudja, M. Maghenem, E. Witrant, D. Georges

Abstract—In this paper, we propose a feedback control strategy to protect vulnerable areas from wildfires. We consider a system of coupled partial differential equations (PDEs) that models heat propagation and fuel depletion in wildfires and study two cases. First, when the wind velocity is known, we design a Neumann-type boundary controller guaranteeing that the temperature of some protected region converges exponentially, in the L^2 norm, to the ambient temperature. Second, when the wind velocity is unknown, we design an adaptive Neumann-type boundary controller guaranteeing the asymptotic convergence, in the L^2 norm, of the temperature of the protected region to the ambient temperature. In both cases, the controller acts along the boundary of the protected region and relies solely on temperature measurements along that boundary. Our results are supported by numerical simulations.

I. INTRODUCTION

Wildfires represent a catastrophic threat, causing widespread destruction across ecosystems, infrastructures, and human settlements. The devastation extends beyond the immediate damage, as wildfires release large amounts of pollutants into the atmosphere, significantly impacting air quality, biodiversity, and soil integrity [9]. As climate change accelerates, the frequency and intensity of these fires are expected to increase, amplifying their effects [2], [12]. This trend makes the ability to predict the spread of heat, and protect vulnerable areas from damage, an urgent global challenge [16].

In response to this growing threat, the physics community has developed advanced models to simulate wildfire dynamics, capturing key phenomena such as heat transfer, fuel depletion, and wind effects. A comprehensive survey of physical and quasi-physical models for wildfire propagation, covering research from 1990 to 2007, is provided in [15]; see also [8] for machine learning-based models. Among the most sophisticated are models based on extended irreversible thermodynamics [14], which explicitly account for the coupling between pyrolysis, gas-phase combustion, and heat transfer mechanisms. While these models offer a deep understanding of wildfire physics, their complexity comes at a cost: Their intricate structure poses significant challenges for real-time estimation and control.

Among the various models available, we consider in this paper the framework proposed in [11], which strikes a

balance between physical relevance and complexity. This model consists of two coupled 2-dimensional PDEs, one governing the transport and diffusion of fire temperature due to fuel combustion, and the other describing the depletion of fuel over time. To the best of our knowledge, this model has been studied by the control community only in [5], [6], where it is used to estimate ignition locations using a sparse sensor network for temperature measurements.

In this paper, we focus on a goal that is different from [5], [6]. We suppose that the wildfire, described by the model from [11], evolves in some domain $\Omega \subset \mathbb{R}_+^2$, with $\mathcal{W} \subset \Omega$ a region to protect. We first consider the case where the wind velocity at the boundary of \mathcal{W} is known, and we design a Neumann-type controller at that location, which ensures that the temperature of \mathcal{W} converges (exponentially) towards the desired ambient level. Next, we suppose that the wind velocity is unknown and bounded, with an unknown upperbound, and we design an adaptive Neumann-type controller which guarantees the boundedness and asymptotic convergence to the ambient temperature of the temperature of \mathcal{W} . The only output available in both cases is the temperature along the boundary of \mathcal{W} .

The rest of the paper is organized as follows. In Section II, we recall the wildfire model in [11], and describe our control objective. In Section III, we state and prove our main results. In Section IV, we illustrate our result by performing a set of numerical simulations. Finally, the paper is finalized by a conclusion and some perspectives.

Notation. Let $\Omega \subset \mathbb{R}_+^2$ be connected. Given $T : \Omega \times [0, +\infty) \rightarrow \mathbb{R}$, with $(x, t) \mapsto T(x, t)$ and $x := [x_1 \ x_2]$, we denote by ΔT the Laplacian of T , defined as $\Delta T := \frac{\partial^2 T}{\partial x_1^2} + \frac{\partial^2 T}{\partial x_2^2}$, where $\frac{\partial^2 T}{\partial x_i^2}$, for $i \in \{1, 2\}$, denotes the second-order partial derivative of T with respect to x_i . Furthermore, we let ∇T be the gradient of T , given by $\nabla T := [\frac{\partial T}{\partial x_1} \ \frac{\partial T}{\partial x_2}]$, where $\frac{\partial T}{\partial x_i}$, for $i \in \{1, 2\}$, is the partial derivative of T with respect to x_i . The divergence of a map $v : \Omega \rightarrow \mathbb{R}^2$, with $v(x) := [v_1(x) \ v_2(x)]$, is defined as $\nabla \cdot v := \frac{\partial v_1}{\partial x_1} + \frac{\partial v_2}{\partial x_2}$. We denote by $a \cdot b$ the scalar product between the two vectors $a, b \in \mathbb{R}^2$, and we let $|a| := \sqrt{a \cdot a}$ be the norm of a . Next, we let $L^2(\Omega; I)$, for a given set $I \subset \mathbb{R}$, be the space of functions $T : \Omega \rightarrow I$ such that $\int_{\Omega} T(x)^2 dx < +\infty$. We also denote by $H^2(\Omega)$ the space of functions $T : \Omega \rightarrow \mathbb{R}$ such that $T, |\nabla T|$, and $\Delta T \in L^2(\Omega; \mathbb{R})$. We let $L_{loc}^2(0, +\infty; H^2(\Omega))$ be the space of functions $T : \Omega \times (0, +\infty) \rightarrow \mathbb{R}$ such that $T(\cdot, t) \in H^2(\Omega)$ for almost all $t \in (0, +\infty)$, and $\int_K \int_{\Omega} (T(x, t)^2 + |\nabla T(x, t)|^2 + (\Delta T(x, t))^2) dx dt < +\infty$ for any compact set $K \subset (0, +\infty)$. We similarly define the space $L_{loc}^2(0, +\infty; L^2(\Omega))$. Finally, a.a. means almost all.

M. C. Belhadjoudja, M. Maghenem, D. Georges are with Univ. Grenoble Alpes, CNRS, Grenoble-INP, GIPSA-lab, F-38000, Grenoble, France (e-mail: mohamed.belhadjoudja, mohamed.maghenem, didier.georges@gipsa-lab.fr).

E. Witrant is with Univ. Grenoble Alpes, CNRS, Grenoble-INP, GIPSA-lab, F-38000, Grenoble, France, and the Departement of Mechanical Engineering, Dalhousie University, Halifax B3H 4R2, Nova Scotia, Canada (e-mail: emmanuel.witrant@gipsa-lab.fr).

II. PROBLEM FORMULATION

A. Wildfire propagation model

We consider in this paper the following system of PDEs

$$\Sigma : \begin{cases} \frac{\partial T}{\partial t} = \varepsilon \Delta T - v \cdot \nabla T + A(Sr(T) - C(T - T_a)) \\ \frac{\partial S}{\partial t} = -C_S Sr(T), \end{cases}$$

where $(T, S) : \Omega \times [0, +\infty) \rightarrow \mathbb{R}_+ \times [0, 1]$ and $\Omega \subset \mathbb{R}_+^2$ is bounded and connected.

The system Σ has been introduced in [11] to model heat propagation and fuel depletion in wildfires. The meaning of each term in Σ is explained below.

- The domain Ω represents the area where the fire evolves.
- t is the time variable.
- T is the temperature of the fire.
- S represents the fuel supply mass fraction, which quantifies the proportion of unburned fuel relative to the total initial fuel mass. In other words, $S(x, t)$ indicates the fraction of fuel that remains available for combustion at a given location $x \in \Omega$ and a given time $t \geq 0$.
- The constant $T_a > 0$ is the ambient temperature.
- The parameter $\varepsilon > 0$ represents the thermal diffusivity, and $\varepsilon \Delta T$ is the diffusion term, governing the spread of heat within the domain.
- The coefficient $A > 0$ corresponds to the maximal temperature increase per unit time when combustion is at its peak, assuming $S := 1$ (ample fuel supply) and negligible cooling effects.
- The constant $C > 0$ characterizes the rate at which heat dissipates into the surroundings.
- $C_S \geq 0$ characterizes the rate at which fuel diminishes relative to its initial amount.
- $v : \Omega \times [0, +\infty) \rightarrow \mathbb{R}^2$, $(x, t) \mapsto v(x, t) = [v_1(x, t) \ v_2(x, t)]$ is the wind velocity, which advects the heat via the advection term $-v \cdot \nabla T$.
- $Sr(T)$ represents the rate at which the fuel is consumed due to burning, with $r(T)$ given by the Arrhenius law

$$r(T) := \begin{cases} \exp^{-\gamma/(T-T_a)} & T > T_a \\ 0 & T \leq T_a, \end{cases}$$

where $\gamma > 0$. We refer to $A(Sr(T) - C(T - T_a))$ as the reaction term.

In this model, the temperature is in Kelvin, the time is in seconds, and the spatial variables are in meter. The units of the coefficients are detailed in [11].

We let $\mathcal{W} \subset \Omega$ be connected, and with a piecewise \mathcal{C}^1 boundary $\partial\mathcal{W}$. Along $\partial\mathcal{W}$, we impose the following Neumann-type boundary condition

$$\frac{\partial T(x, t)}{\partial n(x)} = \kappa(T(x, t) - T_a, x, t) \quad \text{for a.a. } x \in \partial\mathcal{W} \text{ and a.a. } t > 0, \quad (1)$$

where $\kappa : \mathbb{R} \times \partial\mathcal{W} \times [0, +\infty) \rightarrow \mathbb{R}$ will be designed, and $n : \partial\mathcal{W} \rightarrow \mathbb{R}^2$ is the outward-pointing unit normal vector

field to \mathcal{W} ; see [4, Appendix C]. We recall that

$$\frac{\partial T}{\partial n} := n \cdot \nabla T.$$

Furthermore, we suppose that Ω admits a piecewise \mathcal{C}^1 boundary $\partial\Omega$. Along $\partial\Omega \setminus \partial\mathcal{W}$, we impose the following homogeneous Neumann boundary condition

$$\frac{\partial T(x, t)}{\partial \nu(x)} = 0 \quad \text{for a.a. } x \in \partial\Omega \setminus \partial\mathcal{W} \text{ and a.a. } t > 0, \quad (2)$$

where $\nu : \partial\Omega \rightarrow \mathbb{R}^2$ is the outward-pointing unit normal vector field to Ω .

The solutions to Σ under (1)-(2) are understood in the following sense.

Definition 1: A solution to Σ under (1)-(2), starting from the initial condition

$$(T_o, S_o) \in L^2(\Omega; \mathbb{R}_+) \times L^2(\Omega; [0, 1]),$$

is any pair

$$(T, S) \in L_{loc}^2(0, +\infty; H^2(\Omega)) \times L_{loc}^2(0, +\infty; L^2(\Omega))$$

such that the equations in Σ hold for a.a. $x \in \Omega$ and a.a. $t > 0$, (1) and (2) hold for a.a. $t > 0$, a.a. $x \in \partial\mathcal{W}$ and a.a. $x \in \partial\Omega \setminus \partial\mathcal{W}$, respectively, and $(T(x, 0), S(x, 0)) = (T_o(x), S_o(x))$ for a.a. $x \in \Omega$. •

B. Control-design problem

We introduce the deviation

$$\tilde{T} := T - T_a. \quad (3)$$

In this new variable, Σ can be rewritten as:¹

$$\Sigma : \begin{cases} \frac{\partial \tilde{T}}{\partial t} = \varepsilon \Delta \tilde{T} - v \cdot \nabla \tilde{T} + A(S\tilde{r}(\tilde{T}) - C\tilde{T}) \\ \frac{\partial S}{\partial t} = -C_S S\tilde{r}(\tilde{T}), \end{cases}$$

where

$$\tilde{r}(\tilde{T}) := \begin{cases} \exp^{-\gamma/\tilde{T}} & \tilde{T} > 0 \\ 0 & \tilde{T} \leq 0. \end{cases}$$

Furthermore, (1) and (2) become, respectively,

$$\frac{\partial \tilde{T}(x, t)}{\partial n(x)} = \kappa(\tilde{T}(x, t), x, t)$$

for a.a. $x \in \partial\mathcal{W}$ and a.a. $t > 0$,

$$\frac{\partial \tilde{T}(x, t)}{\partial \nu(x)} = 0 \quad \text{for a.a. } x \in \partial\Omega \setminus \partial\mathcal{W} \text{ and a.a. } t > 0.$$

When the wind velocity v is known, we show how to guarantee the following property.

Property 1: Given $S_o \in L^2(\Omega; [0, 1])$, there exists a constant $\alpha > 0$ such that, if (\tilde{T}, S) is a solution to Σ starting from (\tilde{T}_o, S_o) with $\tilde{T}_o \in L^2(\Omega; \mathbb{R})$, we have

$$\int_{\mathcal{W}} \tilde{T}(x, t)^2 dx \leq \left(\int_{\mathcal{W}} \tilde{T}_o(x)^2 dx \right) \exp^{-\alpha t} \quad \forall t \geq 0. \quad (4)$$

¹By abuse of notation, we say that (\tilde{T}, S) is a solution to Σ whenever $(\tilde{T} + T_a, S)$ is a solution to Σ , in the sense of Definition 1.

When the wind velocity is unknown, we show how to guarantee the following property.

Property 2: If (\tilde{T}, S) is a solution to Σ starting from $(\tilde{T}_o, S_o) \in L^2(\Omega; \mathbb{R}) \times L^2(\Omega; [0, 1])$, then

$$\int_{\mathcal{W}} \tilde{T}(x)^2 dx \text{ is bounded and } \lim_{t \rightarrow +\infty} \int_{\mathcal{W}} \tilde{T}(x, t)^2 dx = 0. \quad (5)$$

Remark 1: It is argued in [11] that the wind velocity v can be estimated from atmospheric data or modeled using, e.g., the Navier-Stokes equations. However, both approaches introduce potential inaccuracies, highlighting the need for an adaptive controller to account for imperfect knowledge of the wind velocity. •

Remark 2: Properties 1 and 2 describe how the region \mathcal{W} is protected from the wildfire, albeit in different ways depending on whether the wind velocity is known or not. In Property 1, we essentially guarantee that the region \mathcal{W} is isolated from the wildfire, with the temperature within this region decaying exponentially towards the ambient temperature. On the other hand, in Property 2, when the wind velocity is unknown, we lose the guarantee of exponential decay of the temperature of \mathcal{W} towards the ambient temperature. Without accurate knowledge of the wind velocity, we are not able, with our approach, to fully account for the heat advected from $\Omega \setminus \mathcal{W}$ towards \mathcal{W} . As a result, we no longer guarantee that the protected region \mathcal{W} is isolated from the wildfire. However, we can still ensure that the temperature of \mathcal{W} converges to the ambient temperature as time grows, mitigating the impact of the fire. •

To guarantee Property 1, we require the following assumption.

Assumption 1: We have

$$2AC + \frac{2\varepsilon}{\sup_{x \in \mathcal{W}} |x|^2} - \mathcal{V} - \frac{2A \exp^{-1}}{\gamma} \sup_{x \in \mathcal{W}} |S_o(x)| > 0, \quad (6)$$

where

$$\mathcal{V} := \sup_{x \in \mathcal{W}} |\nabla \cdot v(x)|. \quad (7)$$

Remark 3: Inequality (6) is satisfied when the heat loss coefficient C and the thermal diffusivity ε are sufficiently large. Both coefficients directly influence the magnitude of the stabilizing terms in Σ , with C enhancing heat dissipation, and ε strengthening thermal diffusion. A more interesting aspect is the dependence of (6) on \mathcal{V} , which can be interpreted as the largest value of the wind acceleration in \mathcal{W} . While Assumption 1 does not impose any restrictions on the wind velocity, it does require that the wind acceleration remains relatively small compared to the other positive terms in (6). Intuitively, and informally speaking, a sudden gust or shift in wind direction seems to introduce more complexity to control the spread of wildfires compared to a steady wind. •

To guarantee Property 2, we need, in addition to Assumption 1, the following condition.

Assumption 2: The wind velocity v is bounded along $\partial\mathcal{W}$. That is, there exists a constant $\bar{v} \geq 0$ such that

$$|v(x, t)| \leq \bar{v} \quad \text{for all } (x, t) \in \partial\mathcal{W} \times (0, +\infty). \quad (8)$$

We emphasize that the upperbound \bar{v} on v is not required to be known. •

III. MAIN RESULTS

A. Known Wind Velocity

In this section, we suppose that the wind velocity v along $\partial\mathcal{W}$ is known, and we show how to establish Property 1.

We first introduce the feedback law κ , given by

$$\kappa(\tilde{T}, x, t) := \left[\left(\frac{n(x) \cdot v(x, t) - 2k}{2\varepsilon} \right) - 2 \frac{\sup_{x \in \partial\mathcal{W}} |x|}{\sup_{x \in \mathcal{W}} |x|^2} \right] \tilde{T}, \quad (9)$$

where $k \geq 0$ is a free control gain.

Remark 4: The feedback law κ is constituted of two key terms. The first term, $\tilde{T}(n(x) \cdot v(x, t))/(2\varepsilon)$, counteracts the heat advection across the boundary $\partial\mathcal{W}$ due to wind. Indeed, when $v(x, t) \cdot n(x) > 0$, wind flows inward from $\Omega \setminus \mathcal{W}$ towards \mathcal{W} , bringing external heat into \mathcal{W} . In this case, our controller applies a negative heat flux (cooling) proportional to the incoming flow to counteract this external thermal influence. Conversely, when $v(x, t) \cdot n(x) < 0$, wind flows outward, carrying heat away from \mathcal{W} , potentially making the temperature of \mathcal{W} smaller than the ambient temperature. Here, the controller applies a positive heat flux (heating) to compensate for this heat loss, maintaining a thermal balance. The second term, $\tilde{T}(-k/\varepsilon - 2 \sup_{x \in \partial\mathcal{W}} |x| / \sup_{x \in \mathcal{W}} |x|^2)$, provides damping regardless of wind direction, to regulate the temperature of \mathcal{W} towards the ambient temperature. •

Theorem 1: Suppose that Assumption 1 holds, and let κ be given by (9). Then, Property 1 is verified with

$$\alpha := 2AC + \frac{2\varepsilon}{\sup_{x \in \mathcal{W}} |x|^2} - \mathcal{V} - \frac{2A \exp^{-1}}{\gamma} \sup_{x \in \mathcal{W}} |S_o(x)|. \quad (10)$$

□

Remark 5: Our control strategy has two key features. First, it employs Neumann-type actuation, meaning that we regulate the heat flux at $\partial\mathcal{W}$ rather than directly imposing a temperature on $\partial\mathcal{W}$ (Dirichlet actuation). Neumann boundary control is usually more practical to implement than its Dirichlet counterpart when it comes to thermal systems [1]. E.g., firefighters positioned along $\partial\mathcal{W}$ can activate water sprays, while a control algorithm adjusts in real time their intensity to impose a desired heat flux. Second, our controller is *decentralized* [7], [10], meaning that the value of κ at each location $x \in \partial\mathcal{W}$ depends only on the values of v and T at that location. This is particularly advantageous in environments where state measurements are challenging or costly, such as in wildfire management [3]. •

We follow a Lyapunov-based approach to prove Theorem 1. Specifically, we consider the functional

$$B(\tilde{T}) := \frac{1}{2} \int_{\mathcal{W}} \tilde{T}(x)^2 dx. \quad (11)$$

By differentiating B with respect to time, we obtain

$$\begin{aligned}\dot{B} &= \int_{\mathcal{W}} \tilde{T}(x) \frac{\partial \tilde{T}(x)}{\partial t} dx \\ &= \int_{\mathcal{W}} \tilde{T}(x) \left[\varepsilon \Delta \tilde{T}(x) - v(x) \cdot \nabla \tilde{T}(x) \right. \\ &\quad \left. + A(S(x)\tilde{r}(\tilde{T}(x)) - C\tilde{T}(x)) \right] dx. \quad (12)\end{aligned}$$

In the next set of lemmas, we analyze each term at the right-hand side of (12) in order to derive an appropriate upperbound on \dot{B} . We start by evaluating the contribution of the diffusion term $\varepsilon \Delta \tilde{T}$.

Lemma 1: Along the solutions to Σ , we have

$$\begin{aligned}\int_{\mathcal{W}} \tilde{T}(x) \Delta \tilde{T}(x) dx &\leq -\frac{2}{\sup_{x \in \mathcal{W}} |x|^2} B \\ &\quad + \int_{\partial \mathcal{W}} \left(2 \frac{\sup_{x \in \partial \mathcal{W}} |x|}{\sup_{x \in \mathcal{W}} |x|^2} \right) \tilde{T}(x)^2 d\sigma \\ &\quad + \int_{\partial \mathcal{W}} \frac{\partial \tilde{T}(x)}{\partial n(x)} \tilde{T}(x) d\sigma, \quad (13)\end{aligned}$$

where σ is the surface measure on $\partial \mathcal{W}$; see [4, Appendix C] for the definition of $d\sigma$. \square

Proof: To establish (13), we first use integration by parts to obtain

$$\begin{aligned}\int_{\mathcal{W}} \tilde{T}(x) \Delta \tilde{T}(x) dx &= \int_{\partial \mathcal{W}} \frac{\partial \tilde{T}(x)}{\partial n(x)} \tilde{T}(x) d\sigma \\ &\quad - \int_{\mathcal{W}} |\nabla \tilde{T}(x)|^2 dx. \quad (14)\end{aligned}$$

Next, according to Friedrichs-Poincaré's inequality [13], we have

$$\begin{aligned}\int_{\mathcal{W}} \tilde{T}(x)^2 dx &\leq 2 \sup_{x \in \partial \mathcal{W}} |x| \int_{\partial \mathcal{W}} \tilde{T}(x)^2 d\sigma \\ &\quad + \sup_{x \in \mathcal{W}} |x|^2 \int_{\mathcal{W}} |\nabla \tilde{T}(x)|^2 dx,\end{aligned}$$

which implies that

$$\begin{aligned}- \int_{\mathcal{W}} |\nabla \tilde{T}(x)|^2 dx &\leq -\frac{1}{\sup_{x \in \mathcal{W}} |x|^2} \int_{\mathcal{W}} \tilde{T}(x)^2 dx \\ &\quad + 2 \frac{\sup_{x \in \partial \mathcal{W}} |x|}{\sup_{x \in \mathcal{W}} |x|^2} \int_{\partial \mathcal{W}} \tilde{T}(x)^2 d\sigma. \quad (15)\end{aligned}$$

We obtain (13) by combining (14) and (15). \blacksquare

Next, we evaluate the contribution of advection.

Lemma 2: Along the solutions to Σ , we have

$$\begin{aligned}- \int_{\mathcal{W}} \tilde{T}(x) v(x) \cdot \nabla \tilde{T}(x) dx \\ \leq -\frac{1}{2} \int_{\partial \mathcal{W}} \tilde{T}(x)^2 v(x) \cdot n(x) d\sigma + \mathcal{V} B, \quad (16)\end{aligned}$$

where \mathcal{V} comes from (7). \square

Proof: To establish (16), we first rewrite its left-hand side as

$$\begin{aligned}\int_{\mathcal{W}} \tilde{T}(x) v(x) \cdot \nabla \tilde{T}(x) dx &= \frac{1}{2} \int_{\mathcal{W}} v_1(x) \frac{\partial \tilde{T}(x)^2}{\partial x_1} dx \\ &\quad + \frac{1}{2} \int_{\mathcal{W}} v_2(x) \frac{\partial \tilde{T}(x)^2}{\partial x_2} dx.\end{aligned}$$

Using integration by parts, we obtain

$$\begin{aligned}\int_{\mathcal{W}} v_1(x) \frac{\partial \tilde{T}(x)^2}{\partial x_1} dx &= \int_{\partial \mathcal{W}} \tilde{T}(x)^2 v_1(x) n_1(x) d\sigma \\ &\quad - \int_{\mathcal{W}} \tilde{T}(x)^2 \frac{\partial v_1(x)}{\partial x_1} dx.\end{aligned}$$

Similarly, we have

$$\begin{aligned}\int_{\mathcal{W}} v_2(x) \frac{\partial \tilde{T}(x)^2}{\partial x_2} dx &= \int_{\partial \mathcal{W}} \tilde{T}(x)^2 v_2(x) n_2(x) d\sigma \\ &\quad - \int_{\mathcal{W}} \tilde{T}(x)^2 \frac{\partial v_2(x)}{\partial x_2} dx.\end{aligned}$$

As a consequence,

$$\begin{aligned}\int_{\mathcal{W}} \tilde{T}(x) v(x) \cdot \nabla \tilde{T}(x) dx &= \frac{1}{2} \int_{\partial \mathcal{W}} \tilde{T}(x)^2 v(x) \cdot n(x) d\sigma \\ &\quad - \frac{1}{2} \int_{\mathcal{W}} \tilde{T}(x)^2 (\nabla \cdot v(x)) dx,\end{aligned}$$

which implies (16). \blacksquare

Finally, we analyze the contribution of the term $AS\tilde{r}(\tilde{T})$ coming from the Arrhenius law.

Lemma 3: Along the solutions to Σ , we have

$$\int_{\mathcal{W}} S(x) \tilde{T}(x) \tilde{r}(\tilde{T}(x)) dx \leq \frac{2 \exp^{-1}}{\gamma} \sup_{x \in \mathcal{W}} |S_o(x)| B. \quad (17)$$

\square

Proof: If $\tilde{T} \leq 0$, then $\tilde{r}(\tilde{T}) = 0$ and thus

$$\int_{\mathcal{W}} S(x) \tilde{T}(x) \tilde{r}(\tilde{T}(x)) dx = 0.$$

Now, suppose that $\tilde{T} > 0$. Then,

$$\tilde{T} \tilde{r}(\tilde{T}) = \tilde{T} \exp^{-\gamma/\tilde{T}}.$$

To establish (17), we propose to show that

$$\tilde{T} \exp^{-\gamma/\tilde{T}} \leq \frac{\exp^{-1}}{\gamma} \tilde{T}^2. \quad (18)$$

To do so, we study the variations of the function

$$f(s) := \frac{\exp^{-\gamma/s}}{s} \quad s > 0.$$

By differentiating f , we obtain

$$f'(s) = \frac{\frac{\gamma}{s} - 1}{s^2} \exp^{-\gamma/s}.$$

We note, in particular, that $f'(s) = 0$ if and only if $s = \gamma$. To verify if the latter is a maximum or a minimum point, we differentiate f' to get

$$f''(s) = \left(\frac{-3\gamma + 2s + \frac{\gamma^2}{s} - \gamma}{s^4} \right) \exp^{-\gamma/s}.$$

By evaluating f'' at $s = \gamma$, we obtain

$$f''(\gamma) = -\frac{1}{\gamma^3} \exp^{-1} < 0.$$

As a result, $s = \gamma$ is a maximum point for f , and

$$f(s) \leq f(\gamma) = \frac{\exp^{-1}}{\gamma} \quad \forall s > 0.$$

In particular,

$$\frac{\tilde{T} \exp^{-\gamma/\tilde{T}}}{\tilde{T}^2} = \frac{\exp^{-\gamma/\tilde{T}}}{\tilde{T}} \leq \frac{\exp^{-1}}{\gamma},$$

which further implies (18). Using the latter and the fact that

$$S(x, t) \leq S_o(x) \quad \forall x \in \mathcal{W}, \quad \forall t \geq 0,$$

we get (17). \blacksquare

Now, combining (12), (13), (16), and (17), we obtain

$$\begin{aligned} \dot{B} \leq & -\alpha B + \varepsilon \int_{\partial\mathcal{W}} \kappa(\tilde{T}(x), x) \tilde{T}(x) d\sigma \\ & - \int_{\partial\mathcal{W}} \left(\frac{n(x) \cdot v(x)}{2} \right) \tilde{T}(x)^2 d\sigma \\ & + 2\varepsilon \frac{\sup_{x \in \partial\mathcal{W}} |x|}{\sup_{x \in \mathcal{W}} |x|^2} \int_{\partial\mathcal{W}} \tilde{T}(x)^2 d\sigma. \end{aligned} \quad (19)$$

As a result, under our choice of feedback law in (9), we get

$$\dot{B} \leq -\alpha B - k \int_{\partial\mathcal{W}} \tilde{T}(x)^2 d\sigma, \quad (20)$$

which implies (4).

B. Unknown Wind Velocity

We suppose in this section that the wind velocity v is unknown, and we show how to guarantee Property 2. We propose to set

$$\kappa(\tilde{T}, x, t) := - \left[\left(\frac{\hat{v}(x, t) + 2k}{2\varepsilon} \right) + 2 \frac{\sup_{x \in \partial\mathcal{W}} |x|}{\sup_{x \in \mathcal{W}} |x|^2} \right] \tilde{T}, \quad (21)$$

where $\hat{v} : \partial\mathcal{W} \times (0, +\infty) \rightarrow \mathbb{R}$ is an adaptation parameter governed by

$$\frac{\partial \hat{v}(x, t)}{\partial t} = \frac{\lambda}{2} \tilde{T}(x, t)^2 \quad x \in \partial\mathcal{W}, \quad t > 0, \quad (22)$$

$$\hat{v}(x, 0) = \hat{v}_o(x) \quad x \in \partial\mathcal{W}, \quad (23)$$

with $\lambda > 0$ an adaptation gain and $\hat{v}_o : \partial\mathcal{W} \rightarrow \mathbb{R}_+$.

Theorem 2: Suppose that Assumptions 1 and 2 hold, and let κ be given by (21), with \hat{v} governed by (22)-(23). Then, Property 2 is verified. \square

To prove Theorem 2, we consider the functional

$$\mathcal{Z}(\tilde{T}, \hat{v}) := B(\tilde{T}) + \frac{1}{2\lambda} \int_{\partial\mathcal{W}} (\bar{v} - \hat{v}(x))^2 d\sigma. \quad (24)$$

By differentiating \mathcal{Z} with respect to time, we obtain

$$\dot{\mathcal{Z}} = \dot{B} - \frac{1}{\lambda} \int_{\partial\mathcal{W}} (\bar{v} - \hat{v}(x)) \frac{\partial \hat{v}(x)}{\partial t} d\sigma.$$

Furthermore, using (19), note that we have

$$\begin{aligned} \dot{\mathcal{Z}} \leq & -\alpha B + \varepsilon \int_{\partial\mathcal{W}} \kappa(\tilde{T}(x), x) \tilde{T}(x) d\sigma \\ & - \int_{\partial\mathcal{W}} \left(\frac{n(x) \cdot v(x)}{2} \right) \tilde{T}(x)^2 d\sigma \\ & + 2\varepsilon \frac{\sup_{x \in \partial\mathcal{W}} |x|}{\sup_{x \in \mathcal{W}} |x|^2} \int_{\partial\mathcal{W}} \tilde{T}(x)^2 d\sigma \\ & - \frac{1}{\lambda} \int_{\partial\mathcal{W}} (\bar{v} - \hat{v}(x)) \frac{\partial \hat{v}(x)}{\partial t} d\sigma. \end{aligned}$$

Next, since $|n| = 1$, then

$$- \int_{\partial\mathcal{W}} \left(\frac{n(x) \cdot v(x)}{2} \right) \tilde{T}(x)^2 d\sigma \leq \frac{\bar{v}}{2} \int_{\partial\mathcal{W}} \tilde{T}(x)^2 d\sigma.$$

As a consequence, we obtain

$$\begin{aligned} \dot{\mathcal{Z}} \leq & -\alpha B + \frac{1}{\lambda} \int_{\partial\mathcal{W}} \hat{v}(x) \frac{\partial \hat{v}(x)}{\partial t} d\sigma \\ & + \bar{v} \int_{\partial\mathcal{W}} \left(\frac{\tilde{T}(x)^2}{2} - \frac{1}{\lambda} \frac{\partial \hat{v}(x)}{\partial t} \right) d\sigma \\ & + \varepsilon \int_{\partial\mathcal{W}} \kappa(\tilde{T}(x), x) \tilde{T}(x) d\sigma \\ & + 2\varepsilon \frac{\sup_{x \in \partial\mathcal{W}} |x|}{\sup_{x \in \mathcal{W}} |x|^2} \int_{\partial\mathcal{W}} \tilde{T}(x)^2 d\sigma. \end{aligned}$$

Under the adaptation law in (22), we get

$$\begin{aligned} \dot{\mathcal{Z}} \leq & -\alpha B + \frac{1}{2} \int_{\partial\mathcal{W}} \hat{v}(x) \tilde{T}(x)^2 d\sigma \\ & + \varepsilon \int_{\partial\mathcal{W}} \kappa(\tilde{T}(x), x) \tilde{T}(x) d\sigma \\ & + 2\varepsilon \frac{\sup_{x \in \partial\mathcal{W}} |x|}{\sup_{x \in \mathcal{W}} |x|^2} \int_{\partial\mathcal{W}} \tilde{T}(x)^2 d\sigma. \end{aligned}$$

As a result, under our choice of κ in (21), we obtain

$$\dot{\mathcal{Z}} \leq -\alpha B - k \int_{\partial\mathcal{W}} \tilde{T}(x)^2 d\sigma. \quad (25)$$

The latter implies that \mathcal{Z} is non-increasing. In particular, since $\mathcal{Z} \geq 0$ from (24), then,

$$\lim_{t \rightarrow +\infty} \mathcal{Z}(t) \text{ exists and is finite.}$$

It further implies that

$$\int_0^{+\infty} \dot{\mathcal{Z}}(t) dt < +\infty. \quad (26)$$

Combining (25) and (26), we conclude that

$$\int_0^{+\infty} B(t) dt \leq -\frac{1}{\alpha} \int_0^{+\infty} \dot{\mathcal{Z}}(t) dt < +\infty.$$

Since $B \geq 0$ and $\int_0^{+\infty} B(t) dt < +\infty$, then, by the alternative to Barbalat's lemma in [10, Lemma 3.1], it is enough to show that $\dot{B} \leq M$ for some $M \in \mathbb{R}$ to conclude that B converges asymptotically to zero. To establish the boundedness of \dot{B} from above, first note that, according to (19) and (21), we have

$$\dot{B} \leq \int_{\partial\mathcal{W}} \left(\frac{\bar{v} - \hat{v}(x)}{2} \right) \tilde{T}(x)^2 d\sigma.$$

Since \hat{v} is non-decreasing from (22), and since we have chosen $\hat{v}_o(x) \geq 0$ for all $x \in \partial\mathcal{W}$ in (23), then $\hat{v}(x, t) \geq 0$ for all $x \in \partial\mathcal{W}$ and all $t \geq 0$. As a consequence,

$$\dot{B} \leq \frac{\bar{v}}{2} \int_{\partial\mathcal{W}} \tilde{T}(x)^2 d\sigma \leq \bar{v} B. \quad (27)$$

Now, using (24) and the fact that \mathcal{Z} is non-increasing, we conclude that B is bounded, which further implies, according to (27), that \dot{B} is bounded from above. As a result, B converges asymptotically to zero.

IV. SIMULATION RESULTS

In this section, we illustrate our results via numerical simulations performed in MATLAB. The numerical method is described in the Appendix.

We let $\Omega := [0, L_1] \times [0, L_2]$ and $\mathcal{W} := [2L_1/3, L_1] \times [0, L_2]$, where $L_1, L_2 > 0$. Furthermore, we suppose that

$$v(x, t) := [1 \ 0] \quad \forall x \in \Omega, \quad \forall t > 0.$$

In other words, the wind blows horizontally towards \mathcal{W} at constant speed, advecting the heat from $\partial\Omega \setminus \mathcal{W}$ towards \mathcal{W} .

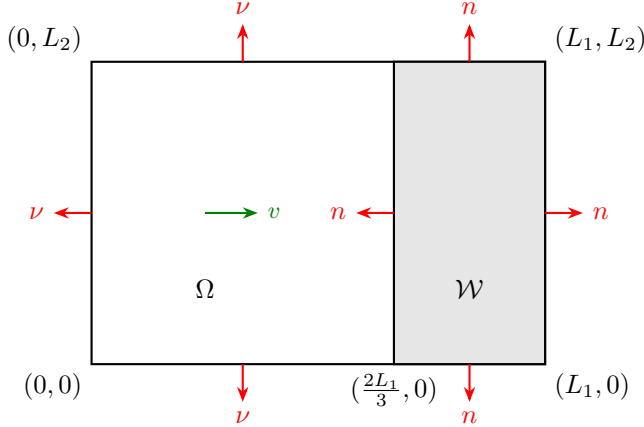
In this setting, the vector field ν is defined as follows

$$\begin{aligned} \nu(0, x_2) &= [-1 \ 0] \quad \forall x_2 \in (0, L_2), \\ \nu(x_1, 0) &= [0 \ -1] \quad \forall x_1 \in (0, L_1), \\ \nu(x_1, L_2) &= [0 \ 1] \quad \forall x_1 \in (0, L_1), \\ \nu(L_1, x_2) &= [1 \ 0] \quad \forall x_2 \in (0, L_2). \end{aligned}$$

Similarly, n is given by

$$\begin{aligned} n\left(\frac{2L_1}{3}, x_2\right) &= [-1 \ 0] \quad \forall x_2 \in (0, L_2), \\ n(x_1, 0) &= [0 \ -1] \quad \forall x_1 \in \left(\frac{2L_1}{3}, L_1\right), \\ n(x_1, L_2) &= [0 \ 1] \quad \forall x_1 \in \left(\frac{2L_1}{3}, L_1\right), \\ n(L_1, x_2) &= [1 \ 0] \quad \forall x_2 \in (0, L_2). \end{aligned}$$

A schematic representation of Ω , \mathcal{W} , ν , n , and v , is shown below.



Since v is constant, then $\mathcal{V} = 0$. Moreover, we note that

$$\sup_{x \in \mathcal{W}} |x|^2 = L_1^2 + L_2^2.$$

As a result, the inequality in Assumption 1 becomes

$$2AC + \frac{2\varepsilon}{L_1^2 + L_2^2} - \frac{2A \exp^{-1}}{\gamma} \sup_{x \in \mathcal{W}} |S_o(x)| > 0, \quad (28)$$

and we select

$$\begin{aligned} A &:= 1.8793 \times 10^2, \quad C := 7.2558 \times 10^{-4}, \\ \varepsilon &:= 2.1360 \times 10^{-1}, \quad \gamma := 5.5849 \times 10^2. \end{aligned}$$

Additionally, the initial fuel supply is assumed to be at its maximum, i.e.,

$$S_o(x) := 1 \quad \forall x \in \Omega.$$

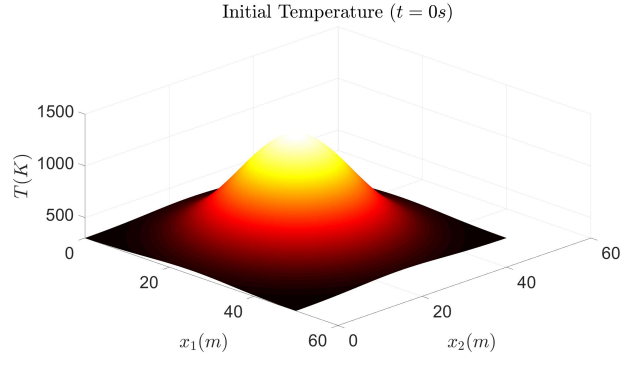


Fig. 1: The initial temperature distribution in (29).

Finally, we set $L_1 = L_2 := 50(m)$. Under the above choice of parameters, Assumption 1 is verified since the left-hand side of (28) is equal to 2.52×10^{-2} .

As in [11], we let the ambient temperature be given by $T_a := 300(K)$. According to Theorem 1, since Assumption 1 holds, then Property 1 is verified, with $\alpha := 2.52 \times 10^{-2}$, if we set κ as in (9). To obtain the expression of κ in this case, first note that

$$\frac{\sup_{x \in \partial\mathcal{W}} |x|}{\sup_{x \in \mathcal{W}} |x|^2} = \frac{\sqrt{L_1^2 + L_2^2}}{L_1^2 + L_2^2} = (L_1^2 + L_2^2)^{-1/2}.$$

Furthermore, we have

$$n(x) \cdot v(x, t) = n(x) \cdot [1 \ 0] = n_1(x).$$

In particular,

$$n(x) \cdot v(x, t) = \begin{cases} -1 & \text{if } x_1 = 2L_1/3 \text{ and } x_2 \in (0, L_2), \\ 1 & \text{if } x_1 = L_1 \text{ and } x_2 \in (0, L_2), \\ 0 & \text{if } x_2 \in \{0, L_2\}. \end{cases}$$

As a consequence, κ becomes

$$\kappa(\cdot) := \begin{cases} \left[\frac{-1 - 2k}{2\varepsilon} - 2(L_1^2 + L_2^2)^{-1/2} \right] \tilde{T} & \text{if } x_1 = 2L_1/3 \text{ and } x_2 \in (0, L_2), \\ \left[\frac{1 - 2k}{2\varepsilon} - 2(L_1^2 + L_2^2)^{-1/2} \right] \tilde{T} & \text{if } x_1 = L_1 \text{ and } x_2 \in (0, L_2), \\ \left[-\frac{k}{\varepsilon} - 2(L_1^2 + L_2^2)^{-1/2} \right] \tilde{T} & \text{if } x_2 \in \{0, L_2\} \\ & \text{and } x_1 \in (2L_1/3, L_1). \end{cases}$$

We select the control gain $k := 1$ for simulations. Moreover, the initial temperature distribution is given by

$$T(x, 0) = T_o(x) := T_a + T_c \exp \frac{-|x - \bar{x}|^2}{2w^2} \quad \forall x \in \Omega, \quad (29)$$

where $T_c := 1000(K)$, $w := 10$, and $\bar{x} := [25 \ 25] (m)$. In Figure 1, we plot T_o .

At the top of Figure 2, we simulate the response of Σ , at $t = 20(s)$, to the boundary condition

$$\frac{\partial \tilde{T}(x, t)}{\partial n(x)} := 0 \quad \text{for a.a. } x \in \partial\mathcal{W}. \quad (30)$$

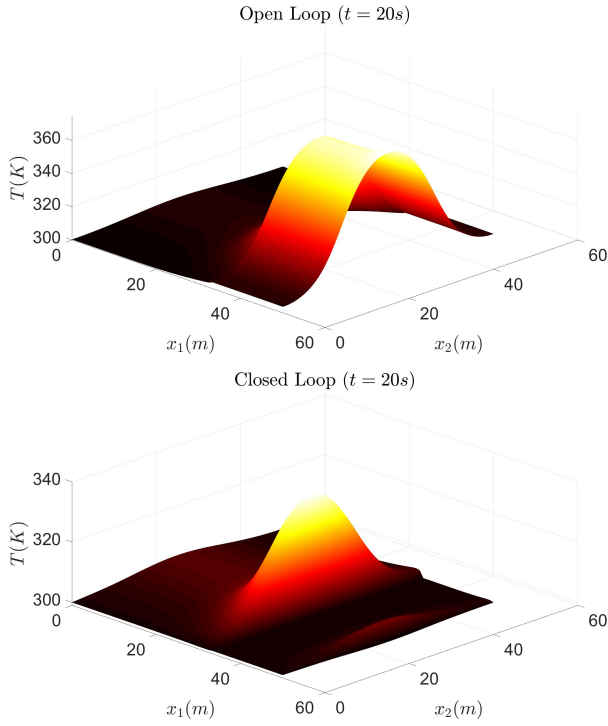


Fig. 2: Response of Σ under (30) (top) vs Response of Σ under (1)-(9) with $k = 1$ (bottom), at $t = 20s$.

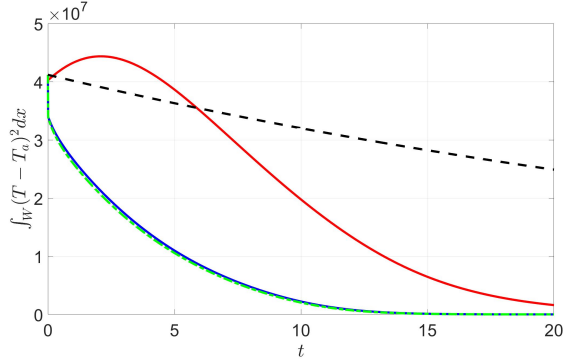


Fig. 3: The squared L^2 norm of the deviation $\tilde{T} = T - T_a$ under (30) (red) vs under (1)-(9) (blue) vs under (1)-(21)-(22)-(23) (green) vs the theoretical bound in the right-hand side of (4) (black).

We can see that the temperature within the region \mathcal{W} is above $T_a = 300(K)$. When closing the loop with our controller (1)-(9), the response of Σ at $t = 20(s)$ is shown at the bottom of Figure 2. We can note that, because of our controller, the temperature within \mathcal{W} converges towards the ambient temperature $T_a = 300(K)$. This is expected from Theorem 1, since $\tilde{T} = T - T_a$ converges to zero in the L^2 norm according to (4). To observe this convergence, we plot in Figure 3 the map $t \mapsto \int_{\mathcal{W}} \tilde{T}(x, t)^2 dx$ under (30), then under (1)-(9). We also plot the theoretical bound on $\int_{\mathcal{W}} \tilde{T}(x)^2 dx$ at the right-hand side of (4). As expected, (4) is verified. Moreover, under (30), although $\int_{\mathcal{W}} \tilde{T}(x)^2 dx$ seems to decay towards zero, it first grows exceeding the right-

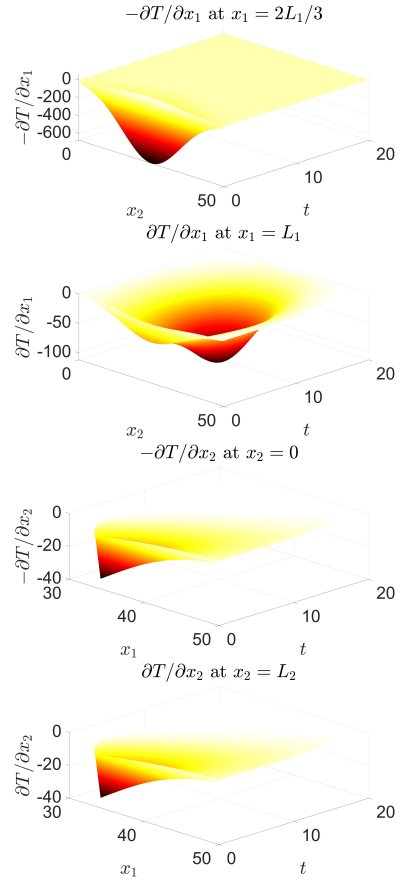


Fig. 4: The controller (1)-(9) along $\partial\mathcal{W}$.

hand side of (4) before starting to decay. Moreover, its decay seems slower than when (1)-(9) is applied.

In Figure 4, we plot the control input in (1)-(9) along each side of $\partial\mathcal{W}$. We can note that the control input is bounded and decreases to zero as time grows. Notably, during the initial iterations, κ is larger along the boundary $x \in \{2L_1/3\} \times (0, L_2)$. This is not surprising, since at that location, the controller needs to counteract the heat advected by the wind from $\partial\Omega \setminus \mathcal{W}$ into \mathcal{W} .

Next, we apply the adaptive controller in (21), with \hat{v} governed by (22)-(23). We select the control gain $k := 1$, the adaptation gain $\lambda := 0.1$, and the initial condition $\hat{v}_o(x) := 0$ for all $x \in \partial\mathcal{W}$. According to Theorem 2, the L^2 norm of \tilde{T} over \mathcal{W} should converge asymptotically to zero, which is confirmed in Figure 6. Interestingly, the decay of $\int_{\mathcal{W}} \tilde{T}(x)^2 dx$ seems faster under our adaptive controller than under our non-adaptive controller in (9). Moreover, in Figure 5, we plot \hat{v} along $\partial\mathcal{W}$. We can see that \hat{v} , while remaining bounded, does not converge to $v = [1 \ 0]$. This is standard in the adaptive control literature, where the convergence of the adaptation parameters to the nominal ones is usually neither guaranteed nor necessary for the convergence of the regulation error to zero [10].

Finally, we consider the case where heat dissipation to the surroundings is negligible, i.e., $C := 0$. Under this condition, Assumption 1 is not satisfied. However, Figure 6 still shows that the temperature of \mathcal{W} converges to $T_a = 300(K)$ under

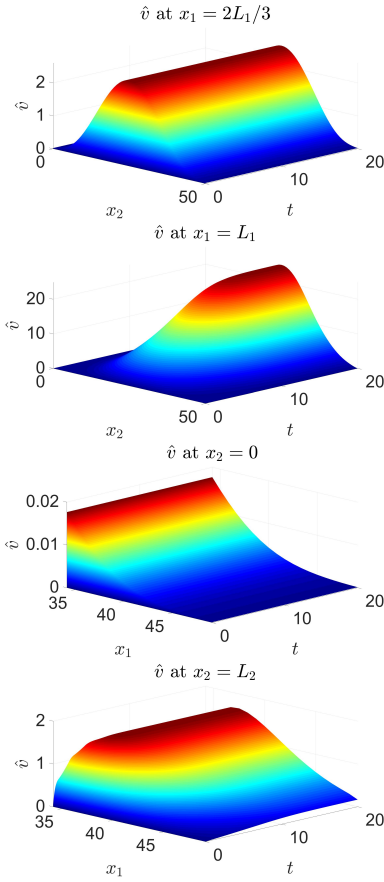


Fig. 5: The adaptation parameter \hat{v} governed by (22)-(23), along $\partial\mathcal{W}$.

both (1)-(9) and (1)-(21)-(22)-(23), whereas under (30), the L^2 norm of \tilde{T} within \mathcal{W} is increasing. These simulation results suggest that Assumption 1, while being sufficient to guarantee the asymptotic convergence of $t \mapsto \int_{\mathcal{W}} \tilde{T}(x, t)^2 dx$ to zero under our controllers, may not be necessary.

V. CONCLUSION AND RESEARCH PERSPECTIVES

In this paper, we considered a well-established model for heat propagation and fuel depletion in wildfires, for which we introduced a feedback-design strategy for regulating the temperature of a given subregion towards the ambient temperature. Specifically, for known wind velocity, we designed a Neumann-type controller guaranteeing the exponential convergence of the temperature to the ambient temperature. For unknown wind velocity, we developed an adaptive Neumann-type controller ensuring the asymptotic convergence of the temperature to the ambient level. Future work will focus on the analysis of the max norm of \tilde{T} , which may allow us to assess the well-posedness of the closed-loop system. It would also be interesting to investigate feedback control of fuel depletion rather than temperature. Finally, a critical challenge would be to account for the intermittency of the actuators, since we may not be able to continuously spray water along the entire boundary of the protected region for all time.

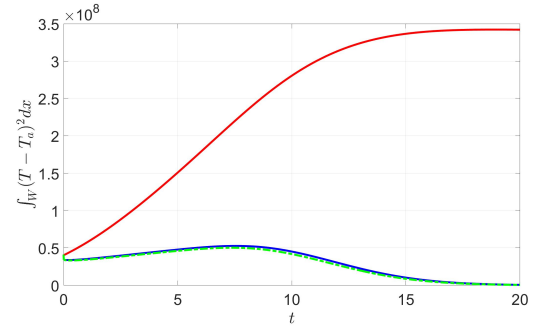


Fig. 6: The squared L^2 norm of \tilde{T} under (30) (red) vs under (1)-(9) (blue) vs under (1)-(21)-(22)-(23) (green), when $C := 0$.

REFERENCES

- [1] A. Balogh, and M. Krstic, "Burgers' equation with nonlinear boundary feedback: H^1 stability, well posedness, and simulation," *Mathematical Problems in Engineering*, 6(2-3), 189-200, 2000.
- [2] S. Bolan et al., "Impacts of climate change on the fate of contaminants through extreme weather events," *Science of The Total Environment*, 909, 168388, 2024.
- [3] C. C. Chan et al., "A Survey on IoT Ground Sensing Systems for Early Wildfire Detection: Technologies, Challenges and Opportunities," in *IEEE Access*, vol. 12, pp. 172785-172819, 2024.
- [4] L. C. Evans, "Partial differential equations," (Vol. 19). *American Mathematical Society*, 1998.
- [5] D. Georges, "A Variational Calculus Approach to Wildfire Monitoring Using a Low-Discrepancy Sequence-Based Deployment of Sensors," in *Proceedings of the 2019 IEEE 58th Conference on Decision and Control (CDC)*, pp. 5912-5917.
- [6] D. Georges, "Towards optimal architectures for hazard monitoring based on sensor networks and crowdsensing," *Integrated disaster risk management journal*, 10(1), 104-146, 2020.
- [7] M. Högberg, and T. R. Bewley, "Spatially localized convolution kernels for decentralized control and estimation of plane channel flow," in *Optimal Control of Boundary Layer Transition*: 123, 2001.
- [8] P. Jain et al., "A review of machine learning applications in wildfire science and management," *Environmental Reviews*, 28(4), 478-505, 2020.
- [9] W. Knorr et al., "Air quality impacts of European wildfire emissions in a changing climate," *Atmospheric Chemistry and Physics*, 16(9), 5685-5703, 2016.
- [10] W. J. Liu, and M. Krstic, "Adaptive control of Burgers' equation with unknown viscosity," *International Journal of Adaptive Control and Signal Processing*, 15(7), 745-766, 2001.
- [11] L. S. Jan Mandel et al., "A wildland fire model with data assimilation," *Mathematics and Computers in Simulation*, 79 (2008) 584-606.
- [12] S. Mansoor et al., "Elevation in wildfire frequencies with respect to the climate change," *Journal of Environmental management*, 301, 113769, 2022.
- [13] K. Rektorys, "The Friedrichs inequality. The Poincaré inequality," in *Variational Methods in Mathematics, Science and Engineering* (pp. 188-198). *Dordrecht: Springer Netherlands*, 1977.
- [14] O. Sero-Guillaume, and J. Margerit, "Modelling forest fires. Part I: A complete set of equations derived by extended irreversible thermodynamics," *International Journal of Heat and Mass Transfer*, 2002, 45(8):1705-1722.
- [15] A. L. Sullivan, "Wildland surface fire spread modelling, 1990-2007. 1: Physical and quasi-physical models," *International Journal of Wildland Fire*, 2009, 18, 349-368.
- [16] D. A. Z. Vazquez, F. Qiu, N. Fan and K. Sharp, "Wildfire Mitigation Plans in Power Systems: A Literature Review," in *IEEE Transactions on Power Systems*, vol. 37, no. 5, pp. 3540-3551, 2022.

APPENDIX

Numerical method

We let $0 = X_o < X_1 < \dots < X_{N_x} = L_1$ and $0 = Y_o < Y_1 < \dots < Y_{N_y} = L_2$, with $N_x = N_y := 80$.

This subdivision of Ω is constructed such that there exists $N^* \in [[0, N_X]]$ with $X_{N^*} = 2L_1/3$. Here, $[[0, N_x]] := \{0, 1, \dots, N_x\}$. Furthermore, we let $\Delta_1 = X_{i+1} - X_i$ for all $i \in [[0, N_X - 1]]$, and $\Delta_2 = Y_{j+1} - Y_j$ for all $j \in [[0, N_Y - 1]]$.

We set $(T(i, j), S(i, j))$, the approximation of $(T(X_i, Y_j), S(X_i, Y_j))$, as a solution to

$$\begin{aligned} \frac{d}{dt}T(i, j) = & \varepsilon \left(\frac{T(i+1, j) - 2T(i, j) + T(i-1, j)}{\Delta_1^2} \right. \\ & + \frac{T(i, j+1) - 2T(i, j-1) + T(i, j-1)}{\Delta_2^2} \\ & - \frac{T(i, j) - T(i-1, j)}{\Delta_1} \\ & + A(S(i, j)r(T(i, j)) - C(T(i, j) - T_a)) \\ & \left. \forall (i, j) \in ([[1, N_x - 1]] \setminus \{N^*\}) \times [[1, N_Y - 1]] \right), \end{aligned} \quad (31)$$

$$\begin{aligned} \frac{d}{dt}S(i, j) = & -C_S S(i, j)r(T(i, j)) \\ & \forall (i, j) \in [[0, N_X]] \times [[0, N_Y]]. \end{aligned} \quad (32)$$

To account for the homogeneous Neumann boundary conditions at $\partial\Omega \setminus \partial\mathcal{W}$, we set

$$\begin{aligned} T(0, j) &= T(1, j) \quad \forall j \in [[0, N_Y]], \\ T(i, 0) &= T(i, 1) \quad \forall i \in [[0, N^* - 1]], \\ T(i, N_Y) &= T(i, N_Y - 1) \quad \forall i \in [[0, N^* - 1]]. \end{aligned}$$

It remains to impose the boundary conditions at $\partial\mathcal{W}$. We distinguish between three different scenarios.

Homogeneous Neumann boundary conditions. To account for (30), we set

$$\begin{aligned} T(N^*, j) &= T(N^* + 1, j) \quad \forall j \in [[0, N_Y]], \\ T(N_X, j) &= T(N_X - 1, j) \quad \forall j \in [[0, N_Y]], \\ T(i, 0) &= T(i, 1) \quad \forall i \in [[N^* + 1, N_X - 1]], \\ T(i, N_Y) &= T(i, N_Y - 1) \quad \forall i \in [[N^* + 1, N_X - 1]]. \end{aligned}$$

The resulting system of ODEs is then integrated using the Euler forward scheme, with the time step $\Delta t := 0.01$.

Non-adaptive controller. To account for (9), we set

$$\begin{aligned} -\frac{T(N^* + 1, j) - T(N^*, j)}{\Delta_1} &= -l_1 \tilde{T}(N^*, j) \quad \forall j \in [[0, N_Y]], \\ \frac{T(N_X, j) - T(N_X - 1, j)}{\Delta_1} &= -l_2 \tilde{T}(N_X, j) \quad \forall j \in [[0, N_Y]], \\ -\frac{T(i, 1) - T(i, 0)}{\Delta_2} &= -l_3 \tilde{T}(i, 0) \\ & \quad \forall i \in [[N^* + 1, N_X - 1]], \\ \frac{T(i, N_Y) - T(i, N_Y - 1)}{\Delta_2} &= -l_3 \tilde{T}(i, N_Y) \\ & \quad \forall i \in [[N^* + 1, N_X - 1]], \end{aligned}$$

where

$$\begin{aligned} l_1 &:= \frac{1}{2\varepsilon} + 2(L_1^2 + L_2^2)^{-1/2} + \frac{k}{\varepsilon}, \\ l_2 &:= l_1 - \frac{1}{\varepsilon}, \\ l_3 &:= l_1 - \frac{1}{2\varepsilon}. \end{aligned}$$

The latter equations can be rewritten as

$$\begin{aligned} T(N^*, j) &= \frac{T(N^* + 1, j)}{1 + \Delta_1 l_1} + \left(\frac{\Delta_1 l_1}{1 + \Delta_1 l_1} \right) T_a \\ & \quad \forall j \in [[0, N_Y]], \\ T(N_X, j) &= \frac{T(N_X - 1, j)}{1 + \Delta_1 l_2} + \left(\frac{\Delta_1 l_2}{1 + \Delta_1 l_2} \right) T_a \\ & \quad \forall j \in [[0, N_Y]], \\ T(i, 0) &= \frac{T(i, 1)}{1 + \Delta_2 l_3} + \left(\frac{\Delta_2 l_3}{1 + \Delta_2 l_3} \right) T_a \\ & \quad \forall i \in [[N^* + 1, N_X - 1]], \\ T(i, N_Y) &= \frac{T(i, N_Y - 1)}{1 + \Delta_2 l_3} + \left(\frac{\Delta_2 l_3}{1 + \Delta_2 l_3} \right) T_a \\ & \quad \forall i \in [[N^* + 1, N_X - 1]]. \end{aligned}$$

As previously, the resulting system of ODEs is integrated using the Euler forward scheme, with $\Delta t := 0.01$.

Adaptive controller. Finally, we suppose that κ is given by (21) with \hat{v} governed by (22)-(23). We discretize (31) and (32) using the Euler forward scheme with the time step $\Delta t := 0.01$. Furthermore, to account for (1), we let $T(i, j, n)$ and $\hat{v}(i, j, n)$, the approximation of $T(X_i, Y_j, n\Delta t)$ and $\hat{v}(X_i, Y_j, n\Delta t)$ respectively, verify, along $\partial\mathcal{W}$, the following equations

$$\begin{cases} -\frac{\tilde{T}(N^* + 1, j, n) - \tilde{T}(N^*, j, n)}{\Delta_1} = -\left[\frac{\hat{v}(N^*, j, n-1)}{2\varepsilon} \right. \\ \quad \left. + \frac{\lambda\Delta t}{4\varepsilon} + \frac{\tilde{T}(N^*, j, n)^2 + 2k}{2\varepsilon} + 2(L_1^2 + L_2^2)^{-1/2} \right] \tilde{T}(N^*, j, n), \\ \hat{v}(N^*, j, n) = \hat{v}(N^*, j, n-1) + \frac{\lambda\Delta t}{2} \tilde{T}(N^*, j, n)^2, \\ \quad \forall j \in [[0, N_Y]], \\ \frac{\tilde{T}(N_X, j, n) - \tilde{T}(N_X - 1, j, n)}{\Delta_1} = -\left[\frac{\hat{v}(N_X, j, n-1)}{2\varepsilon} \right. \\ \quad \left. + \frac{\lambda\Delta t}{4\varepsilon} + \frac{\tilde{T}(N_X, j, n)^2 + 2k}{2\varepsilon} + 2(L_1^2 + L_2^2)^{-1/2} \right] \tilde{T}(N_X, j, n), \\ \hat{v}(N_X, j, n) = \hat{v}(N_X, j, n-1) + \frac{\lambda\Delta t}{2} \tilde{T}(N_X, j, n)^2, \\ \quad \forall j \in [[0, N_Y]], \\ -\frac{\tilde{T}(i, 1, n) - \tilde{T}(i, 0, n)}{\Delta_2} = -\left[\frac{\hat{v}(i, 0, n-1)}{2\varepsilon} \right. \\ \quad \left. + \frac{\lambda\Delta t}{4\varepsilon} + \frac{\tilde{T}(i, 0, n)^2 + 2k}{2\varepsilon} + 2(L_1^2 + L_2^2)^{-1/2} \right] \tilde{T}(i, 0, n), \\ \hat{v}(i, 0, n) = \hat{v}(i, 0, n-1) + \frac{\lambda\Delta t}{2} \tilde{T}(i, 0, n)^2, \\ \quad \forall i \in [[N^* + 1, N_X - 1]], \end{cases}$$

$$\begin{cases} \frac{\tilde{T}(i, N_Y, n) - \tilde{T}(i, N_Y - 1, n)}{\Delta_2} = - \left[\frac{\hat{v}(i, N_Y, n - 1)}{2\varepsilon} \right. \\ \left. + \frac{\lambda\Delta t}{4\varepsilon} + \frac{\tilde{T}(i, N_Y, n)^2 + 2k}{2\varepsilon} + 2(L_1^2 + L_2^2)^{-1/2} \right] \\ \times \tilde{T}(i, N_Y, n), \\ \hat{v}(i, N_Y, n) = \hat{v}(i, N_Y, n - 1) + \frac{\lambda\Delta t}{2} \tilde{T}(i, N_Y, n)^2, \\ \forall i \in [[N^* + 1, N_X - 1]]. \end{cases}$$

In each of the four latter cases, we obtain a cubic polynomial equation in the variable \tilde{T} at $\partial\mathcal{W}$. Specifically, we get

$$\begin{aligned} \tilde{T}(N^*, j, n)^3 + p_1(N^*, j)\tilde{T}(N^*, j, n) + q_1(N^* + 1, j) &= 0 \\ \forall j \in [[0, N_Y]], \\ \tilde{T}(N_X, j, n)^3 + p_1(N_X, j)\tilde{T}(N_X, j, n) + q_1(N_X - 1, j) &= 0 \\ \forall j \in [[0, N_Y]], \\ \tilde{T}(i, 0, n)^3 + p_2(i, 0)\tilde{T}(i, 0, n) + q_2(i, 1) &= 0 \\ \forall i \in [[N^* + 1, N_X - 1]], \\ \tilde{T}(i, N_Y, n)^3 + p_2(i, N_Y)\tilde{T}(i, N_Y, n) + q_2(i, N_Y - 1) &= 0 \\ \forall i \in [[N^* + 1, N_X - 1]], \end{aligned}$$

where

$$\begin{aligned} p_m(i, j) &:= \frac{4\varepsilon}{\lambda\Delta t} \left(\frac{\hat{v}(i, j, n - 1) + 2k}{2\varepsilon} + 2(L_1^2 + L_2^2)^{-1/2} \right. \\ &\quad \left. + \frac{1}{\Delta_m} \right), \\ q_m(i, j) &:= -\frac{4\varepsilon}{\lambda\Delta t\Delta_m} \tilde{T}(i, j, n), \end{aligned}$$

and for $m \in \{1, 2\}$. For each of the above cubic polynomial equations, the discriminant is nonnegative since $\hat{v} \geq 0$. As a result, each cubic polynomial equation admits a unique real root given by Cardano's formula

$$\begin{aligned} T(N^*, j, n) &= \\ &\sqrt[3]{-\frac{q_1(N^* + 1, j)}{2} + \sqrt{\frac{q_1(N^* + 1, j)^2}{4} + \frac{p_1(N^*, j)^3}{27}}} \\ &+ \sqrt[3]{-\frac{q_1(N^* + 1, j)}{2} - \sqrt{\frac{q_1(N^* + 1, j)^2}{4} + \frac{p_1(N^*, j)^3}{27}}} \\ &+ T_a \quad \forall j \in [[0, N_Y]], \end{aligned}$$

$$\begin{aligned} T(N_X, j, n) &= \\ &\sqrt[3]{-\frac{q_1(N_X - 1, j)}{2} + \sqrt{\frac{q_1(N_X - 1, j)^2}{4} + \frac{p_1(N_X, j)^3}{27}}} \\ &+ \sqrt[3]{-\frac{q_1(N_X - 1, j)}{2} - \sqrt{\frac{q_1(N_X - 1, j)^2}{4} + \frac{p_1(N_X, j)^3}{27}}} \\ &+ T_a \quad \forall j \in [[0, N_Y]], \end{aligned}$$

$$\begin{aligned} T(i, 0, n) &= \sqrt[3]{-\frac{q_1(i, 1)}{2} + \sqrt{\frac{q_1(i, 1)^2}{4} + \frac{p_1(i, 0)^3}{27}}} \\ &+ \sqrt[3]{-\frac{q_1(i, 1)}{2} - \sqrt{\frac{q_1(i, 1)^2}{4} + \frac{p_1(i, 0)^3}{27}}} \\ &+ T_a \quad \forall i \in [[N^* + 1, N_X - 1]], \end{aligned}$$

$$\begin{aligned} T(i, N_Y, n) &= \\ &\sqrt[3]{-\frac{q_1(i, N_Y - 1)}{2} + \sqrt{\frac{q_1(i, N_Y - 1)^2}{4} + \frac{p_1(i, N_Y)^3}{27}}} \\ &+ \sqrt[3]{-\frac{q_1(i, N_Y - 1)}{2} - \sqrt{\frac{q_1(i, N_Y - 1)^2}{4} + \frac{p_1(i, N_Y)^3}{27}}} \\ &+ T_a \quad \forall i \in [[N^* + 1, N_X - 1]]. \end{aligned}$$